

FEA APPROACH FOR PREDICTING THE DYNAMIC BEHAVIOUR OF CORK-RUBBER COMPOSITES

Lopes, H.*; Silva, S. P.** & Machado, J.*

* University of Minho, MEtRICs Research Center, Campus of Azurém, 4800-058 Guimarães, Portugal

** Amorim Cork Composites, Rua Comendador Américo Ferreira Amorim, 260, 4535-186 Mozelos VFR, Portugal

E-Mail: id7466@alunos.uminho.pt

Abstract

Cork-rubber composites can be applied as isolation blocks for systems under dynamic compressive loading. Under the same loading conditions, different geometries of the same cork-rubber material present distinct static and dynamic compression behaviour. To reduce the number of experimental tests for different geometries, a methodology, employing finite element analysis (FEA), is proposed. Considering static and dynamic experimental results of a 60 Shore A cork-rubber squared cross section specimen, an equivalent single degree of freedom model is derived, and its data is introduced on FEA to determine the dynamic behaviour of samples with different dimensions. Dynamic stiffness and natural frequency results showed a good agreement between experimental and numerical approaches for a standard sample and specimens with different thicknesses and areas, especially when considering static deformation due to preload. The developed study allows the prediction of the dynamic behaviour of different dimension samples through FEA output, based only on experimental testing.

(Received in January 2022, accepted in May 2022. This paper was with the authors 1 month for 1 revision.)

Key Words: Cork-Rubber Composites, Dynamic Compression, Dynamic Stiffness, FEA, Natural Frequency, Shape Factor

1. INTRODUCTION

Cork-rubber composites are elastomeric materials composed of a rubber compound matrix filled with cork granules. One of the application fields of cork-rubber materials is its use as isolation blocks in buildings, heavy machinery or other systems subjected to dynamic loadings [1, 2]. Materials with similar functions include synthetic rubbers, foams, thermoplastic elastomers, among others.

Cork-rubber isolation blocks are employed to diminish vibration transmission between the source and surrounding environment. Some systems, which contemplate this solution, are subjected to compression. Regarding loading type, during the development of these products, two requirements must be met: (1) supporting loads without presenting signs of creep or failure, and (2) having appropriate dynamic characteristics to prevent transmission of vibration between structures [3].

One of the considered properties in the design of cork-rubber isolation blocks is mechanical behaviour when subjected to compressive loads. Elastomeric elements, for vibration isolation, can have different shapes, and, usually, are bonded to rigid plates that transmit the load to the elastomer [4]. Considering compression loading and bonded contact, the mechanical behaviour of a material depends mainly on its geometry. To describe this effect, shape factor (s_f) is used, relating loaded and free to bulge areas [5, 6]. Several works, considering this dependence between shape factor or geometry and static mechanical behaviour, had been developed [5, 7-9], including an approach developed for cork-rubber composites under small strain compression [10].

Another characteristic to consider throughout the design of isolation blocks is the response to dynamic loadings. Like other elastomers, cork-rubber materials exhibit viscoelastic behaviour and the system response varies according to static preload, temperature, vibration

frequency and amplitude [11]. Generally, the dynamic mechanical properties of an elastomer can be assessed by different methods, like free, forced non-resonance or resonance vibrations [12]. In the case of isolation blocks, it is common to evaluate the materials based on standard DIN 53513 [13]. Also, to characterize materials, the dynamic stiffness coefficient can be determined, through the ratio between dynamic and static stiffness [4]. Therefore, it is expected that different geometry samples – varying on shape factor, for example – of the same material, besides showing distinct compression behaviour with a bonded contact, also provide different dynamic responses.

Nowadays, recurring to computational resources, it is possible to model different kinds of materials and simulate the mechanical behaviour according to the desired inputs. The application of previous data, for simulation purposes [14] or to develop models based on machine learning techniques [15], is currently being explored as a tool to determine new materials' properties. Other approaches consist of the development of specific models able to adapt to different materials characteristics without the need to rely on huge experimental datasets [16].

Finite elements analysis is one of the applied techniques to study elastomers' behaviour at static and dynamic loading conditions [11, 17-20]. Besides elastomers and cork-rubber composites, the application of FEA as part of the study of other bio-based materials has also been addressed in several works [21, 22]. Regarding elastomers' static behaviour, as presented in [10], Young's modulus can provide a relationship between shape factor and apparent compression modulus. Based on the results obtained by [10], an approach, recurring to FEA, was developed to find the dynamic characteristics of cork-rubber specimens obtained through the experimental method based on DIN 53513 [13].

This article presents a case study regarding 60 Shore A cork-rubber samples with a squared cross section. Based on dynamic compression tests of one specimen, an equivalent single degree of freedom model (SDOF) was derived. Considering a SDOF system and the effect of shape factor on compression behaviour, finite element analysis was employed to determine the dynamic mechanical properties of specimens with different dimensions. To validate the approach, numerical and experimental results from several samples were compared.

The present study is organized in the following order. Firstly, a general description of the methodology applied in this research is introduced. Experimental methods, considerations about the finite element analysis and its relation to providing the same dynamic mechanical properties given by experimental tests are presented. The results section includes the experimental dynamic results of a sample with 60×60×10 mm that served as the base for predicting the dynamic behaviour of other specimens. A comparison between the standard sample experimental results with the application of the presented methodology is also presented. Next, the prediction of the dynamic behaviour of samples with various dimensions through FEA outputs and its comparison with previous experimental data is given. Finally, conclusions are presented.

2. MATERIALS AND METHODS

The proposed methodology, in this article, focuses on the determination of dynamic mechanical properties of cork-rubber specimens with different dimensions, based on the obtained data from experimental testing of one sample of the same cork-rubber material, designated beyond this point as "standard sample".

Overall, in this research, two different methods were applied to determine the dynamic mechanical properties of cork-rubber composites: an experimental test based on DIN 53513 [13] and finite element analysis. In the following sections, descriptions are provided about the setup and data treatment of results for each employed method.

A scheme of the proposed approach in this study is presented in Fig. 1. According to the standard sample's results, an equivalent SDOF model is derived to determine the input data for numerical simulation. With the results obtained by the FEA approach, the dynamic properties, based on standard DIN 53513 [13], can be calculated. The dynamic properties studied were dynamic stiffness, dynamic compression modulus and natural frequency of a system composed of a cork-rubber composite as a combination of elastic and viscous components.

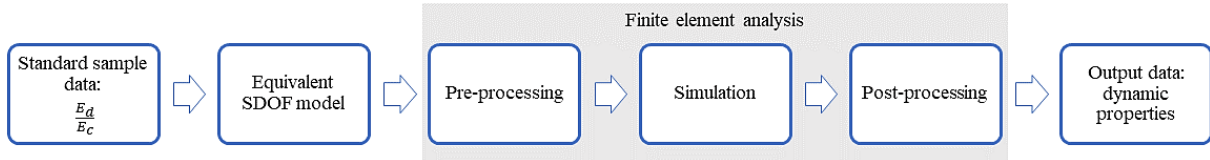


Figure 1: Proposed methodology to determine the dynamic properties of samples with different dimensions.

2.1 Experimental tests

Dynamic and quasi-static compression tests were performed on several specimens of a cork-rubber composites material with hardness around 60 Shore A. The tested samples had squared cross sections and different dimensions. Quasi-static compression test was performed first in a universal testing machine at 5 mm/min until strain between 25 and 30 % was achieved. To achieve the behaviour of isolation blocks under the application of compressive loading, no lubricant was applied between the sample and compression plates, simulating a frictional contact. Each sample was successively compressed three times, with only the third test being recorded. From this test, load-displacement data was retrieved, and apparent compression modulus (E_c in Pa) was calculated according to Eq. (1).

$$E_c = \frac{\sigma}{\varepsilon} \quad (1)$$

where σ is stress [Pa] and ε is strain. Because the studied cork-rubber composites present a linear behaviour until 10 % strain [10], which corresponds to the range of compression deformation considered in the design of vibration isolators [4], the apparent compression modulus was calculated based on the stress value correspondent to that point.

After the quasi-static compression test, specimens were subjected to a dynamic compression test performed by a servo-hydraulic fatigue machine with a load cell of 25 kN. Based on standard DIN 53513 [13], the test consisted of imposing a sinusoidal load with a mean level correspondent to a specific stress and amplitude of 10 % of the mean load applied at a constant exciting frequency during 150 cycles. Each sample was subjected to different stress levels until a maximum of 3 MPa, after being pre-conditioned at the same exciting frequency with a mean load correspondent to 1.8 MPa with 10 % load amplitude. Data obtained from the last twenty cycles were retrieved and analysed. Parameters like dynamic stiffness (k_t in N/m), dynamic compression modulus (E_d in Pa) and natural frequency of the system (f_{nt} in Hz), when subjected to each stress level, were calculated according to Eqs. (2), (3) and (4), respectively.

$$k_t = \frac{F_a}{d_a} \cos \delta \quad (2)$$

$$E_d = \frac{k_t T}{A} \quad (3)$$

$$f_{nt} = \frac{1}{2\pi} \sqrt{\frac{k_t g}{F_m}} \quad (4)$$

where F and d are load [N] and displacement [m], δ is the phase shift between load and displacement, T and A are the initial thickness [m] and cross section area [m²] of the specimen, a and m are subscripts for the amplitude and mean values of the sinusoidal curves, t is the subscript indicative of experimental testing and g is the gravitational acceleration [m/s²].

Also, with the results from quasi-static and dynamic compression tests, the ratio between dynamic and apparent compression modulus was calculated at different stress ranges.

2.2 Finite element analysis

To obtain the properties considered in the experimental method, Eqs. (2) to (4), harmonic analysis was conducted using FEA. Simulations were performed using the Harmonic Response module of Ansys Workbench. The finite element model was composed of a continuous solid block, representing the cork-rubber specimen. A mass point was added to the top surface of the block and its value correspond to a certain stress level imposed on a cork-rubber specimen during dynamic experimental tests. A fixed support condition was considered on the opposite surface of the block. The numerical analysis consisted of simulating the application of a sinusoidal load with an amplitude of 10 % of the mean applied load, recording as output the displacement amplitude of the system at the value of the exciting frequency used in experimental tests of the standard sample. The experimental setup and 3-D finite element model are presented in Figs. 2 a and 2 b, respectively.

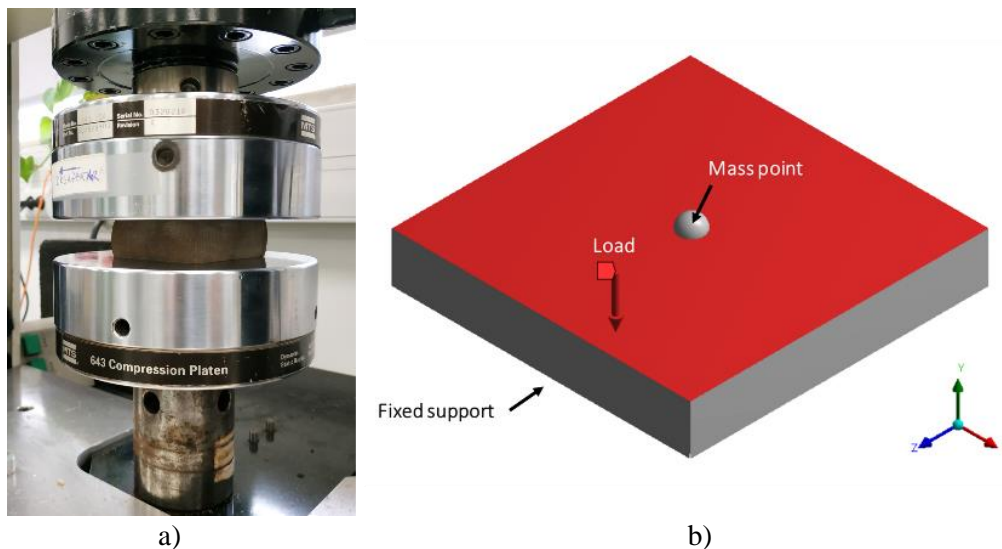


Figure 2: Dynamic compression of a cork-rubber composite sample: a) experimental setup; b) finite element model.

The stiffness and damping characteristics of the system were entered in the simulation as properties of the cork-rubber material. For each stress level, the equivalent Young's modulus (E_{0eq} in Pa) was determined and used as input for the simulation. The methodology and procedure to calculate Young's modulus are presented in section 2.3. Density and Poisson's ratio of the cork-rubber composite were also introduced as inputs. Density corresponded to 1075 kg/m³. The value of Poisson's ratio was 0.31, as considered in [10]. Due to the hysteretic nature of the material analysed, and loss factor (η) values for the studied material being very low, the damping ratio (ζ) was calculated based on the phase shift obtained by experimental results, as described in Eq. (5). This parameter was considered constant throughout the stress range since previous results regarding the studied material reveal to be very similar.

$$\zeta = \frac{\eta}{2} = \frac{\tan \delta}{2} \quad (5)$$

2.3 Determination of equivalent properties for FEA

The general procedure to determine equivalent Young's modulus values to be introduced in finite element analysis is presented in Fig. 3. The effect of the variation of frequency, strain amplitude and temperature on the properties of cork-rubber composites was not considered in this study.

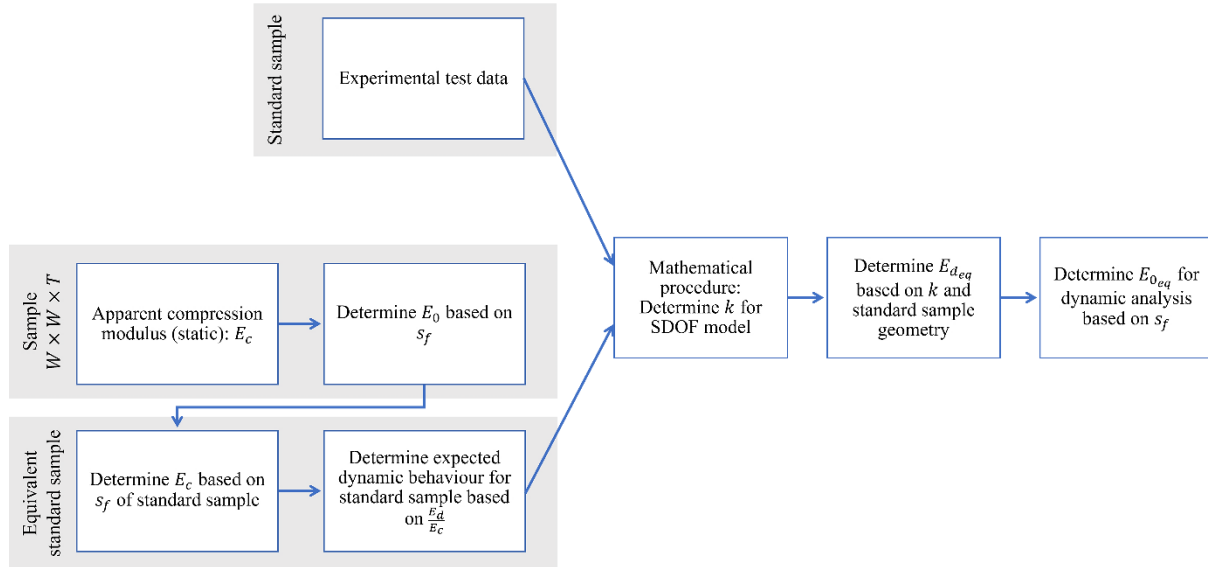


Figure 3: Procedure to find equivalent Young's modulus.

Using the experimental results of a standard sample, the inputs for the mathematical procedure to determine equivalent Young's Modulus values, include the displacement amplitude obtained for each stress level. As some variability of static behaviour between samples with different shape factors can occur, it was also considered the use of the ratio between dynamic and static compression modulus as input data. The ratio between the two moduli can be calculated based on the experimental results obtained for the standard sample. Based on the apparent compression modulus of another sample with different dimensions, the apparent compression modulus and expected dynamic testing results of an equivalent standard sample (with the same intrinsic properties) are determined, based on the relation between shape factor and Young's modulus (E_0 in Pa) [10]. These are the inputs to be introduced for the mathematical procedure to determine the correspondent equivalent Young's modulus values.

The mathematical procedure consists of finding a value for the spring constant of a single degree of freedom model, equivalent to the one obtained or expected to be obtained by experimental testing of a standard sample. In a SDOF model composed of a mass (m in kg), spring and damper, excited by a sinusoidal external load, the displacement amplitude (X_a in m), in steady state, is calculated by Eq. (6).

$$X_a = \frac{F_a}{k} Q \quad (6)$$

where k represents the spring constant [N/m] and Q is the amplification factor calculated from Eq. (7).

$$Q = \frac{1}{\sqrt{(1 - \beta^2)^2 + (2\zeta\beta)^2}} \quad (7)$$

where β represents the ratio between exciting frequency (f in Hz) and natural frequency (f_n in Hz). The phase angle and natural frequency of the SDOF model can be calculated accordingly to Eqs. (8) and (9), respectively.

$$\tan \delta = \frac{2\zeta\beta}{1 - \beta^2} \quad (8)$$

$$f_n = \frac{1}{2\pi} \sqrt{\frac{k}{m}} \quad (9)$$

At each stress level, to obtain the same dynamic properties results of the experimental test through harmonic analysis, the SDOF model's displacement amplitude (X_a) must be equalled to the displacement obtained through the dynamic testing method (d_a). An iterative numeric procedure was employed to determine the value of k , that fulfils this condition, according to Eqs. (10) and (11).

$$X_a = d_a \quad (10)$$

$$X_a = \frac{F_a}{k} \left(\sqrt{(1 + \tan^2 \delta) \left(1 - \frac{4\pi^2 f^2 F_m}{kg} \right)^2} \right)^{-1} \quad (11)$$

The iterative process to find the solution for the stiffness value was performed using Solver add-in from Microsoft Excel. With the value of stiffness, an equivalent dynamic compression modulus (E_{deq} in Pa) can be determined, considering the geometry of the standard sample. Then, according to the shape factor and using the dynamic compression modulus value, an equivalent Young's modulus can be determined based on the results of [10].

2.4 Dynamic properties of samples with different dimensions

Considering the same cork-rubber composite but specimens with different dimensions from the standard sample, after determining the equivalent Young's modulus for each stress level, dynamic properties were determined based on the results obtained from finite element analyses. The loading conditions corresponded to the same stress levels considered in a standard sample: equal stress level with 10 % load amplitude. Also, the change of thickness on the block due to static deformation must be considered, as described by Gent [12]. Considering the linear behaviour at static compression, the value of dynamic stiffness corresponding to an experimental test, using FEA output, is given by the expression presented in Eq. (12). The dynamic compression modulus and natural frequency are also calculated according to Eqs. (3) and (4).

$$k_t = \left(1 - \frac{F_m}{E_c A} \right) \frac{F_a}{X_{aFEA}} \cos \delta \quad (12)$$

where X_{aFEA} is the displacement amplitude [m] given by the finite element analysis.

3. RESULTS AND DISCUSSION

For a standard sample, the results obtained by dynamic compression experimental tests are presented first. The results obtained through finite element analysis for the standard sample were analysed and compared against experimental results to validate the developed approach. Based on the dynamic experimental results of the standard sample, predictions about the dynamic mechanical properties of the same cork-rubber material with different dimensions are also presented. Simulation results related to squared cross section blocks with different thicknesses and different areas were analysed and compared against previous experimental data.

3.1 Standard sample

Ten standard samples with a cross section of 60×60 mm and 10 mm thickness (shape factor of 1.5) were characterized in terms of static and dynamic behaviour between 0.5 and 3 MPa. As depicted in Fig. 4, the increase of the stress, imposed in the sample, affects the dynamic compression modulus. In terms of natural frequency, it is possible to verify that natural frequency decreases and tends to stabilize at higher stress levels. There is a combined effect due to the simultaneous variation of dynamic stiffness and the compression level employed on the sample, which affects the natural frequency results.

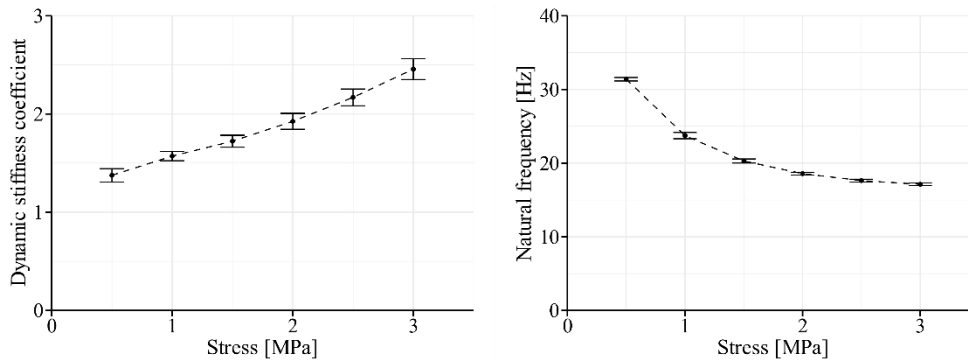


Figure 4: Results of a dynamic experimental test of a 60×60×10 mm sample.

Based on the displacement amplitude observed at each stress level, the stiffness values correspondent to an equivalent single degree of freedom model were determined. Equivalent dynamic compression modulus and Young's modulus were also calculated based on the stiffness value obtained by the applied mathematical procedure. Since the shape factor of the standard sample was 1.5, Young's modulus value to be inserted on finite element analysis was determined according to the expression presented in Eq. (13) [10]:

$$E_{0eq} = 0.775 E_{deq} \quad (13)$$

Table I presents data relative to the experimental dynamic test and the results obtained by the mathematical procedure to achieve equivalent Young's modulus values, considering the conditions of the experimental test.

Table I: Dynamic test conditions and results of equivalent SDOF model.

Experimental data				Equivalent SDOF model		
Exciting freq. f (Hz)	$\tan \delta$	Stress σ (MPa)	Load amplitude F_a (N)	E_d (MPa)	E_{deq} (MPa)	E_{0eq} (MPa)
5	0.09	0.5	180	19.9	20.4	15.8
		1	360	22.8	23.8	18.4
		1.5	540	25.0	26.5	20.5
		2	720	27.9	29.9	23.2
		2.5	900	31.4	33.9	26.3
		3	1080	35.6	38.6	29.9

The displacement amplitude results, obtained by FEA, were used to calculate the expected dynamic stiffness and natural frequency according to Eqs. (2) and (4), respectively. Results of dynamic stiffness and natural frequency were compared with experimental data as presented in Fig. 5. As is possible to verify, the results from FEA are within the standard deviation observed in experimental tests, showing a good agreement between the two methods applied in this study. The values of relative error were below 2 % for natural frequency and less than 4 % for dynamic stiffness.

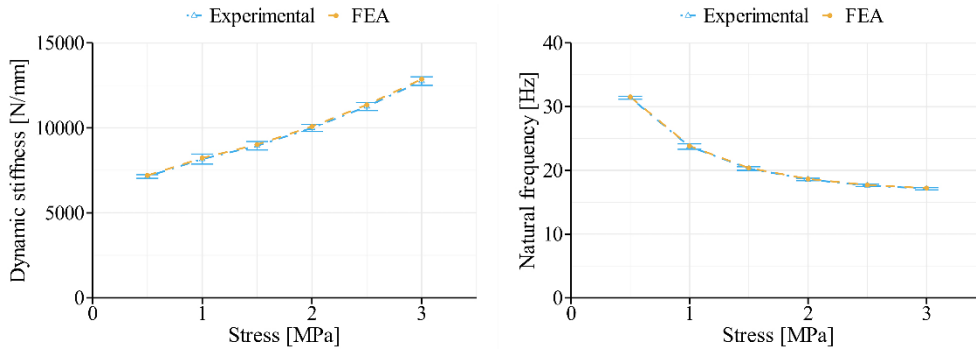


Figure 5: Comparison between dynamic stiffness and natural frequency results obtained by experimental and simulation approaches.

3.2 Samples with different thickness

Specimens with equal cross section area of the standard sample and different thicknesses were considered to evaluate the performance of the simulation approach. To do that, previous experimental results regarding other different thickness samples of the same cork-rubber composite were used. Due to some differences in terms of static behaviour between these samples and the standard sample presented in previous sections, other standard specimens, with similar static behaviour to the first samples, were considered for the equivalent SDOF model, according to the scheme presented in Fig. 3. Table II shows the apparent compression modulus of equivalent standard samples considering previous quasi-static experimental results of different thickness samples. Based on the dynamic stiffness coefficient obtained from the standard sample experimental results (Fig. 4 a), the dynamic behaviour of equivalent standard samples was also determined. The values of dynamic compression modulus (E_d) of the correspondent standard samples for each case are presented in Fig. 6.

Table II: Apparent compression modulus of standard sample $60 \times 60 \times 10$ mm considering static compression data of other specimens.

Thickness T (mm)	Shape factor s_f	Results from compression tests		Equivalent standard sample ($s_f = 1.5$)
		E_c (MPa)	E_0 (MPa)	E_c (MPa)
25	0.6	4.93	4.20	5.42
30	0.5	5.60	4.87	6.28
50	0.3	5.57	5.12	6.61

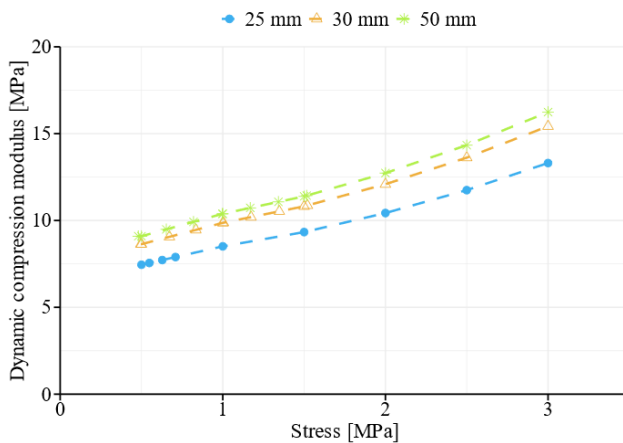


Figure 6: Dynamic compression modulus of standard samples considering static compression data from other specimens.

Other input conditions to determine the values of Young’s modulus to be entered in the FEA were the same ones considered in the experimental testing of the standard sample, except for the value of exciting frequency. In this case, previous experimental tests of higher thickness samples were performed at 15 Hz. To be able to compare the results obtained by FEA with this data, an exciting frequency of 15 Hz was introduced in the mathematical procedure to retrieve the input values for FEA simulation.

The results of the expected dynamic stiffness and natural frequency between 0.5 and 3 MPa, based on the simulation results for samples with thickness values presented in Table II, are represented in Fig. 7. Comparison with available previous experimental results was only possible inside the stress range considered. Maximum errors occurred for the sample with 25 mm thickness (shape factor of 0.6) with values of 3.1 % for natural frequency and 8.5 % for dynamic stiffness. Differences could be related to some small variations of some conditions during the experimental test, such as load amplitude, or due to the results related to the use of linear interpolation to determine the apparent compression modulus for a sample of shape factor 0.6.

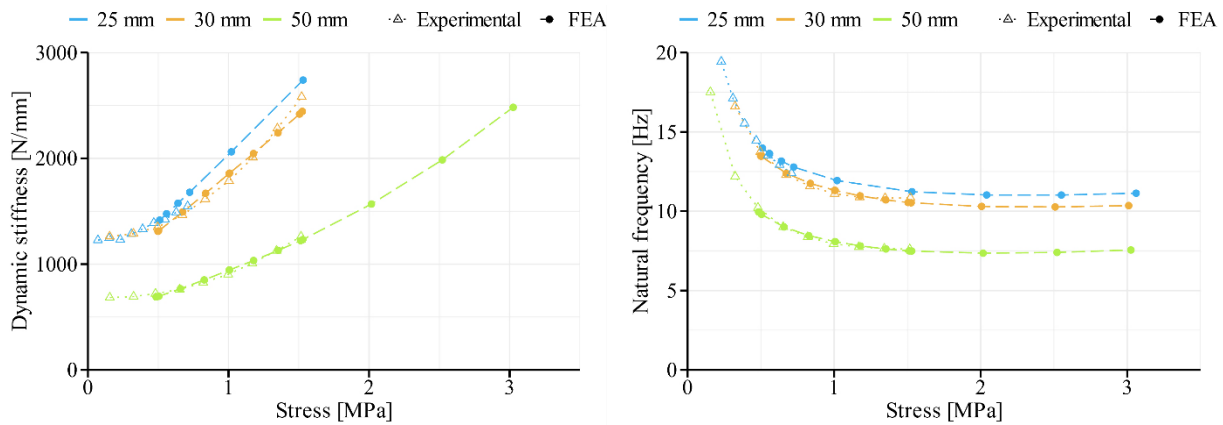


Figure 7: Comparison between dynamic stiffness and natural frequency results obtained by experimental and simulation approaches for samples with other thicknesses.

3.3 Samples with different cross section areas and thicknesses

The dynamic behaviour of samples with different cross section areas and thicknesses was also determined through the FEA approach. Previous experimental results of cork-rubber squared blocks samples with cross section 150×150 mm were also used for comparison. For this case, a similar compression behaviour between the three geometries was assumed considering Young’s modulus of 4.4 MPa. As described in the previous section, an equivalent standard sample with similar static behaviour was considered for the equivalent SDOF model. The conditions and results of the mathematical procedure for the determination of the equivalent SDOF model are presented in Table III.

Table III: Conditions and results of equivalent SDOF model, considering the standard sample with 60×60×10 mm.

Experimental data					Equivalent SDOF model	
Exciting freq. f (Hz)	$\tan \delta$	Stress σ (MPa)	Load amplitude F_a (N)	E_d (MPa)	E_{deq} (MPa)	E_{0eq} (MPa)
15	0.09	0.56	201.6	8.0	13.1	10.1
		0.96	345.6	8.9	17.6	13.6
		1.52	547.2	9.9	23.7	18.3
		2	720	11.0	29.1	22.6

In order to determine the dynamic properties of a specimen with a cross section of 150×150 mm, finite element analyses were conducted based on the equivalent Young's modulus and damping ratio presented in Table III. For each stress level, the mass point value was adapted to achieve the same stress imposed in a $60 \times 60 \times 10$ mm sample. Load amplitude values corresponded to 10 % of the mean load considered for the larger cross section. The results obtained by the numerical approach were compared against previous experimental data (Fig. 8).

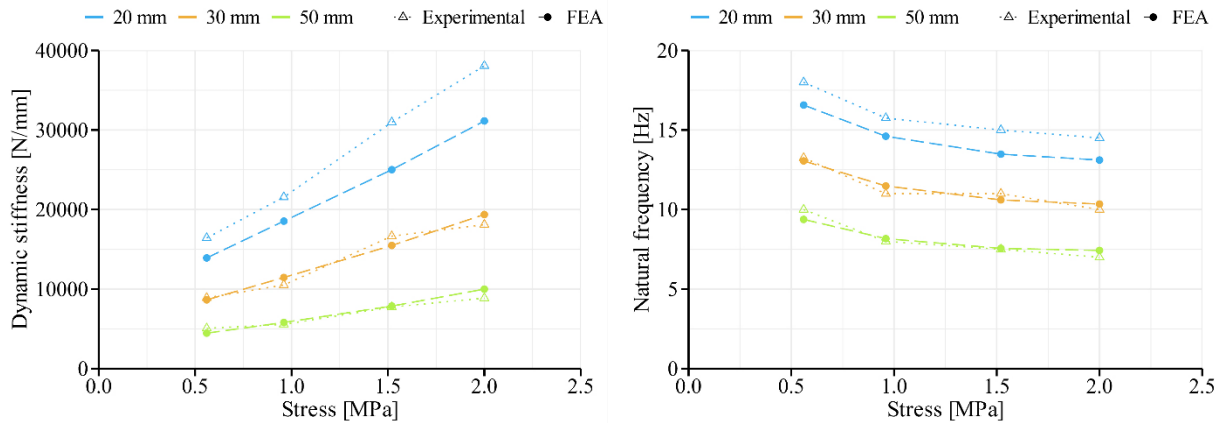


Figure 8: Comparison between dynamic stiffness and natural frequency results obtained by experimental and simulation approaches for specimens with a cross section area of 150×150 mm.

As is possible to observe, generally, results from the two approaches are in good agreement. However, some differences are noticed for the sample with 20 mm thickness, with a maximum error of 10.1 % for natural frequency and 19.2 % related to dynamic stiffness. In terms of absolute error, the differences between experimental and approach-based natural frequency results were around 1.5 Hz. These differences could be due to the variability between material compounds in terms of dynamic stiffness coefficient or variation of some conditions during the experimental test, such as load amplitude or sample dimensions that could impact the results, especially in terms of dynamic stiffness.

4. CONCLUSION

A new methodology, based on the results from finite element analysis, was developed to determine the dynamic mechanical properties of cork-rubber composites used as isolation blocks for vibration control. Thus, a prediction about the results given by an experimental test based on DIN 53513 can be assessed by knowing the dynamic behaviour of a single sample (standard sample). The application of the presented methodology can provide a valuable tool during the design of specific solutions, and it could allow the reduction of experimental testing of different samples of the same cork-rubber composite material. Also, with the presented approach, it may be possible to save time, materials and resources for obtaining results related to a specific composite during its development stage.

Generally, the results obtained for a 60 Shore A cork-rubber material with isotropic behaviour revealed a good agreement with experimental results. Differences below 5 % were registered between the developed approach and experimental tests regarding the use of a standard sample with $60 \times 60 \times 10$ mm. Based on the ratio between dynamic and apparent compression moduli obtained from the standard sample, predictions were performed about the dynamic stiffness and natural frequency for specimens with the same cross section shape but different dimensions. For most cases, these results showed a good agreement, with a maximum error below 10 % for natural frequency and 20 % for dynamic stiffness, with previous

experimental data from other samples. Differences could be related to the variation of some experimental factors, like amplitude load, sample dimensions, cork-rubber compounds used for different samples or related to the assumptions of the methodology.

Regarding this research topic, future works could include the evaluation of the implementation of this methodology in cork-rubber materials with different hardness, cross section shapes or geometries. Also, the utilization of other geometries as standard samples should be evaluated, as well as the effect of the variability of cork-rubber compounds on the results obtained by the numerical approach. Considering other aspects of the mechanical behaviour, such as non-linearity at high strains or anisotropy, the assumptions of the study should also be reconsidered. Another possible research topic can also focus on the application of data-based techniques for properties prediction, such as artificial intelligence methods, and consequently, the development and application of an extensive and representative database for this purpose.

ACKNOWLEDGEMENTS

The authors are grateful to Amorim Cork Composites for providing all materials and resources for this study. Helena Lopes was supported by scholarship SFRH/BD/136700/2018 financed by Fundação para a Ciência e Tecnologia (FCT-MCTES) and co-funded by European Social Fund through Norte2020 (Programa Operacional Regional Norte). This work has been supported by the FCT within the RD Units Project Scope: UIDP/04077/2020 and UIDB/04077/2020.

REFERENCES

- [1] Gil, L. (2009). Cork composites: a review, *Materials*, Vol. 2, No. 3, 776-789, doi:[10.3390/ma2030776](https://doi.org/10.3390/ma2030776)
- [2] Silva, S. P.; Sabino, M. A.; Fernandes, E. M.; Correlo, V. M.; Boesel, L. F.; Reis, R. L. (2005). Cork: properties, capabilities and applications, *International Materials Reviews*, Vol. 50, No. 6, 345-365, doi:[10.1179/174328005X41168](https://doi.org/10.1179/174328005X41168)
- [3] Jones, D. I. G. (2001). *Handbook of Viscoelastic Vibration Damping*, John Wiley & Sons, Chichester
- [4] Rivin, E. I. (2003). *Passive Vibration Isolation*, ASME Press, New York, doi:[10.1115/1.80187X](https://doi.org/10.1115/1.80187X)
- [5] Gent, A. N.; Lindley, P. B. (1959). The compression of bonded rubber blocks, *Proceedings of the Institution of Mechanical Engineers*, Vol. 173, No. 1, 111-122, doi:[10.1243/PIME_PROC_1959_173_022_02](https://doi.org/10.1243/PIME_PROC_1959_173_022_02)
- [6] Schaefer, R. J. (2002). Mechanical properties of rubber, Harris, C. M.; Piersol, A. G. (Eds.), *Harris' Shock and Vibration Handbook*, 5th edition, McGraw-Hill, New York
- [7] Horton, J. M.; Tupholme, G. E.; Gover, M. J. C. (2002). Axial loading of bonded rubber blocks, *Journal of Applied Mechanics*, Vol. 69, No. 6, 836-843, doi:[10.1115/1.1507769](https://doi.org/10.1115/1.1507769)
- [8] Lindley, P. B. (1979). Compression moduli for blocks of soft elastic material bonded to rigid end plates, *The Journal of Strain Analysis for Engineering Design*, Vol. 14, No. 1, 11-16, doi:[10.1243/03093247V14I011](https://doi.org/10.1243/03093247V14I011)
- [9] Williams, J. G.; Gamonpilas, C. (2008). Using the simple compression test to determine Young's modulus, Poisson's ratio and the Coulomb friction coefficient, *International Journal of Solids and Structures*, Vol. 45, No. 16, 4448-4459, doi:[10.1016/j.ijsolstr.2008.03.023](https://doi.org/10.1016/j.ijsolstr.2008.03.023)
- [10] Lopes, H.; Silva, S.; Machado, J. (2020). Analysis of the effect of shape factor on cork-rubber composites under small strain compression, *Applied Sciences*, Vol. 10, No. 20, Paper 7177, 10 pages, doi:[10.3390/app10207177](https://doi.org/10.3390/app10207177)
- [11] Koblar, D.; Boltežar, M. (2016). Evaluation of the frequency-dependent Young's modulus and damping factor of rubber from experiment and their implementation in a finite-element analysis, *Experimental Techniques*, Vol. 40, No. 1, 235-244, doi:[10.1007/s40799-016-0027-7](https://doi.org/10.1007/s40799-016-0027-7)
- [12] Gent, A. N. (2012). *Engineering with Rubber*, 3rd edition, Carl Hanser Verlag, München, doi:[10.3139/9783446428713](https://doi.org/10.3139/9783446428713)

- [13] DIN 53513 (1990). *Determination of the viscoelastic properties of elastomers on exposure to forced vibration at non-resonant frequencies*, Beuth Verlag, Berlin
- [14] Banić, M.; Stamenković, D.; Miltenović, A.; Jovanović, D.; Tica, M. (2020). Procedure for the selection of rubber compound in rubber-metal springs for vibration isolation, *Polymers*, Vol. 12, No. 8, Paper 1737, 15 pages, doi:[10.3390/polym12081737](https://doi.org/10.3390/polym12081737)
- [15] Serban, F. M.; Grozav, S.; Ceclan, V.; Turcu, A. (2020). Artificial neural networks model for springback prediction in the bending operations, *Technical Gazette*, Vol. 27, No. 3, 868-873, doi:[10.17559/TV-20141209182117](https://doi.org/10.17559/TV-20141209182117)
- [16] Rosnitschek, T.; Hueter, F.; Alber-Laukant, B. (2020). FEM-based modelling of elastic properties and anisotropic sinter shrinkage of metal EAM, *International Journal of Simulation Modelling*, Vol. 19, No. 2, 197-208, doi:[10.2507/IJSIMM19-2-509](https://doi.org/10.2507/IJSIMM19-2-509)
- [17] Bolmsvik, Å.; Linderholt, A. (2015). Damping elastomers for wooden constructions – dynamic properties, *Wood Material Science & Engineering*, Vol. 10, No. 3, 245-255, doi:[10.1080/17480272.2015.1046920](https://doi.org/10.1080/17480272.2015.1046920)
- [18] Cole, D.; Forrester, S.; Fleming, P. (2018). Mechanical characterisation and modelling of elastomeric shockpads, *Applied Sciences*, Vol. 8, No. 4, Paper 501, 13 pages, doi:[10.3390/app8040501](https://doi.org/10.3390/app8040501)
- [19] Fahimi, S.; Baghani, M.; Zakerzadeh, M.-R.; Eskandari, A. (2018). Developing a visco-hyperelastic material model for 3D finite deformation of elastomers, *Finite Elements in Analysis and Design*, Vol. 140, 1-10, doi:[10.1016/j.finel.2017.10.009](https://doi.org/10.1016/j.finel.2017.10.009)
- [20] Zhou, T.; Wu, Y.-F.; Li, A.-Q. (2018). Numerical study on the ultimate behavior of elastomeric bearings under combined compression and shear, *KSCE Journal of Civil Engineering*, Vol. 22, 3556-3566, doi:[10.1007/s12205-018-0949-y](https://doi.org/10.1007/s12205-018-0949-y)
- [21] Bose, R.; Kandavel, A. (2021). Mechanical characterization and structural attributes of biohybrid composites derived using hemp, bamboo, and jute fibres: an alternative approach in the application of natural fibres in automobile parts, *Strojniški vestnik – Journal of Mechanical Engineering*, Vol. 67, No. 10, 534-544, doi:[10.5545/sv-jme.2021.7272](https://doi.org/10.5545/sv-jme.2021.7272)
- [22] Zhang, X.; Wang, J.; Meng, Q.; Yu, M.; Zhang, Z.; Guo, Z. (2021). Coal rock breaking simulation and cutting performance analysis of disc cutters, *Technical Gazette*, Vol. 28, No. 5, 1755-1761, doi:[10.17559/TV-20210423115559](https://doi.org/10.17559/TV-20210423115559)